arXiv:1402.5244v3 [physics.optics] 3 Aug 2015

Fluorescence Excitation by Enhanced Plasmon Upconversion under Continuous Wave Illumination

Mehmet Emre Tasgin,[1] Ildar Salakhutdinov,[2,3] Dania Kendziora,[4] Musa Kurtulus Abak,[2,5] Deniz Turkpence,[6] Luca Piantanida,[7,8] Ljiljana Fruk,[4,9] Marco Lazzarino,[7,10] and Alpan Bek[2,3,5,*]

[1] *Institute of Nuclear Sciences, Hacettepe University, Beytepe, 06800 Ankara, Turkey*
[2] *Center for Solar Energy Research and Applications (GÜNAM), Middle East Technical University, Dumlupınar Blvd. 1, 06800, Ankara, Turkey*
[3] *Physics Department, Middle East Technical University, Dumlupınar Blvd. 1, 06800 Ankara, Turkey*
[4] *DFG-Centre for Functional Nanostructures, Karlsruhe Institute of Technology, Wolfgang Gaede Str. 1, 76131 Karlsruhe, Germany*
[5] *Micro and Nanotechnology Program, Middle East Technical University, Dumlupınar Blvd. 1, 06800 Ankara, Turkey*
[6] *Department of Physics, Koç University, İstanbul, Sarıyer 34450, Turkey*
[7] *CNR-IOM, Area Science Park, 34149 Trieste, Italy*
[8] *Graduate School of Nanotechnology, Department of Physics, University of Trieste, 34127 Trieste, Italy*
[9] *Department of Chemical Engineering and Biotechnology, University of Cambridge, Pembroke Street, Cambridge CB2 3RA, United Kingdom*
[10] *CBM S.c.r.l., Area Science Park, Basovizza, 34149 Trieste, Italy*

(Dated: August 4, 2015)

We demonstrate effective background-free continuous wave nonlinear optical excitation of molecules that are sandwiched between asymmetrically constructed plasmonic gold nanoparticle clusters. Near infrared photons are converted to visible plasmon oscillations through efficient plasmonic second harmonic generation. Molecules absorb the visible plasmons and fluoresce. Our theoretical model and simulations demonstrate that Fano resonances may be responsible for being able to observe nonlinear conversion using a continuous wave light source. We show that nonlinearity enhancement of plasmonic nanostructures via coupled quantum mechanical oscillators such as molecules can be several orders larger as compared to their classical counterparts.

PACS numbers: xx

I. INTRODUCTION

Finding a possibility to control the activation of a single molecule is interesting since it paves the way to realize logic devices as small as molecules. This can be achieved by carefully designed devices which can interface a single molecule and interact with it at the same size scale. Such devices can be of electrical, magnetic or optical origin [1] and may induce changes in the properties of a single or few molecules which can act as switching registers for data processing or data storage at the nanometer scale. Electrical devices at the single molecule size level include break-junctions [2], scanning tunnelling microscope tip junctions [3], and molecular landers [4]. Optical devices that can interface a single molecule among an ensemble of many molecules are yet lacking. The main difficulty lies in the diffraction limit of practically $\sim$ 150-180 nm focal size for a wavelength of 600 nm light. Compared to a few nm sizes of individual molecules, unambiguous activation of single molecules by means of absorption of light can only be possible for a device prepared from a sparse ensemble of molecules. Thanks to advancement in near-field optical instrumentation technology this main difficulty can be circumvented as the near-field light intensities typically have a very strong nonlinear dependence on distance (from $\sim r^3$ to $\sim r^6$). Strongly confined, highly intense fields of light called "hot spots", can be achieved by engineering the nanoscale environment of a single molecule. By utilizing plasmonic resonances of nanoscale metal structures, such spots can be arranged to occupy from a few down to a single molecule. Nevertheless in these schemes, a broad far-field background component of the same activation wavelength is inevitably superposed on to the near-field of the nanoparticles. This imposes limitations on single molecule activation experiments to be performed with high fidelity. Due to quantum nature of light, even a weak linear optical background signal can give rise to activation of a single molecule as long as the excitation signal is within the absorption / activation spectrum of the molecule.

In an attempt to overcome the linear background problem, a nonlinear optical scheme namely SHG can be used to address a single molecule. One approach to activate a single molecule is to use optical up-conversion of two simultaneously incident NIR photons to create a single visible photon by the plasmonic activity of a metal nanoparticle cluster. It was shown earlier that asymmetric metal nanostructures are important for achieving second-order nonlinear optical response from plasmonic activity [5]. An efficient second harmonic (SH) active plasmonic metal nanostructure can be constructed by composing a cluster of colloidal metal nanoparticles with two different sizes [6]. It is of essence to break the centro-symmetry of the cluster in order to have a nonvanishing second order

* bek@metu.edu.tr

susceptibility, $\chi^{(2)}$. The strategy in this approach is to minimize the volume of nonlinear photoactivation by selectively activating the single or probably a few molecules which is/are located in the vicinity of the gap between the nanoparticles of such an asymmetric cluster. The photoactivation of a small number of molecules can be monitored by selecting the sandwiched molecules to possess a linear fluorescent nature and thereby absorb light only at the SH frequency and not possess a significant two-photon fluorescence cross-section at the irradiated frequency.

In the absorption spectrum of hybrid structures that are made of coupled classical and quantum oscillators of charge such as a plasmonic gold nanoparticle (AuNP) attached to a single molecule (or a quantum dot, etc.) path interference effects similar to Fano resonances are observed [7–10]. The two absorption paths for the classical oscillator, induced by the hybridization with the quantum oscillator, can interfere destructively yielding a cancellation of the polarization on the plasmonic response for some frequencies [11]. In our recent theoretical and numerical studies using 3D simulations with retardation effects [12, 13], we have demonstrated that path interference schemes can be adopted to gain control over the nonlinear frequency conversion processes emerging in plasmonic resonators. By appropriately choosing the level spacing of the quantum oscillator (i.e. choosing the right molecule), one can either enhance or suppress the frequency conversion process by several orders of magnitude. An enhancement in the nonlinear response emerges whenever the path interference is arranged to cancel the nonresonant terms, thereby bringing the conversion to resonance. Enhancements in frequency conversion due to Fano resonances of interacting classical nanoparticles have already been studied numerically [14] and observed experimentally [15–17]. In a recent experimental study [15] an enhancement factor of 25 is reported.

In this paper, we show that fluorescent molecules with absorption bans in visible part of the spectrum can be brought to fluoresce under continuous wave (cw) near infra red (NIR) excitation. This is shown to be possible by a physical process which involves strong plasmonic enhancement of SHG. We prepare two different clusters, i) 12 nm sized AuNPs decorated with fluorescent molecules (Fig.1 (a)-(b)) and ii) bare AuNPs of sizes between 50 120 nm. We observe that upon cw excitation with NIR laser these two clusters do not express SHG or fluorescence. However when the two clusters are brought together (Fig. 1 (c)-(d)), we observe visible fluorescence from the molecules.

We argue that fluorescence is realized by absorption of the up-converted plasmon excitation from the AuNP clusters. We consider the SHG process, since the converted wavelength lies within the linear absorption spectrum of the molecule (Fig. 2). We show that further enhancement of SHG process in plasmonic clusters can emerge due to enhanced path interference effects.

We introduce a simple theoretical model where a plasmonic converter interacts with a quantum emitter (QE) which has a longer excitation lifetime. We examine the steady-state solutions for this model. We show how the enhancement may emerge [see Eq. (8)]. As an exaple system, we obtain the spectral position of the plasmon modes of three coupled AuNPs with different sizes 100, 70 and 12 nm, where the molecule is attached to the 12 nm one. Our simulation is the exact solution of 3D Maxwell's equations (taking retardation effects into account) which is performed using MNPBEM [18]. We demonstrate that our theoretical model can yield SH enhancement factors as large as 1000. In difference to previous calculations [12], here, we consider coupling of the molecule to two visible plasmon modes, into which SH oscillations (2ω) can emerge.

The experimental details on preparation of such a sample and excitation measurement results are provided in section II. The details on our theoretical model and the simulations carried out in line with the model are presented in section III. Finally in section IV we discuss our findings and conclude.

II. EXPERIMENT

A. Experimental Methods

AuNPs were synthesized according to literature [19]. Glassware was cleaned with aqua regia, thoroughly washed with water and dried at 70^{o}C. In a three-neck flask 25 mL chloroauric acid (1 mM, 25 mol, 1 eq.) was heated under reflux to 100^{o}C. After addition of 2.50 mL trisodium citrate (38.8 mM, 97 μmol, 3.88 eq.) the solution was stirred for 1 h and cooled to room temperature. Resulting AuNP were analyzed with UV-Vis spectroscopy and transmission optical microscopy (TEM). The diameter was determined to 11.7 $\pm$ 0.96 nm. Concentration of AuNP was estimated using a literature known extinction coefficient of $\epsilon_{450nm} = 6.15.10^7$ $M^{-1}cm^{-1}$ for citrate coated AuNP [20].

Larger, nondecorated AuNPs of 50-70 nm size were synthesized following a revised version of the well-known Turkevich method [21–24]. Sodium citrate (0.86 mM) was dissolved in 100 mL of milliQ water and the solution was heated up to 100^{o}C without refluxing system. At the boiling point a solution of $HAuCl_4$ 3 H_2O (1 mL, 0.04 mM) was added and the mixture was left boiling for 5 min before cooling down to room temperature (RT).

DNA-modified AuNP were formed by ligand exchange with thiolated oligonucleotides as described in an earlier publication [25]. Briefly, 100 μL thiolated oligonucleotide (100 μM, 10 nmol, 1 eq.) were reduced with 60 μL dithiothreitol (DTT, 1 M, 60 μmol, 6000 eq.) over night at 37^{o}C. The reaction mixture was purified with gel filtration using NAP5 und NAP10 columns (GE Healthcare). To the resulting solution 1 mL citrate-stabilised AuNP (30 nM, 30 pmol, 0.003 eq.) were added and incubated

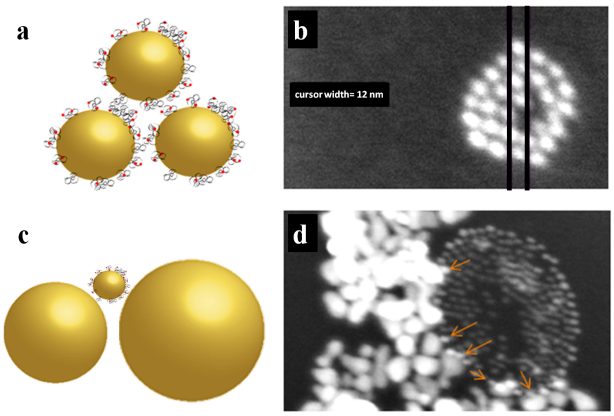

Figure 1. (color online) Symmetric and asymmetric AuNP clusters. (a) The EYFP decorated Au nanoparticle, (b) An SEM image of a symmetric cluster of such nanoparticles indicating the size of the Au nanoparticles of ∼12 nm, (c) The sketch of an asymmetric AuNP dimer with a single/few molecule/s in the gap, (d) An SEM image of a surface prepared using both types of nanoparticles displaying such asymmetric clusters as indicated by arrows.

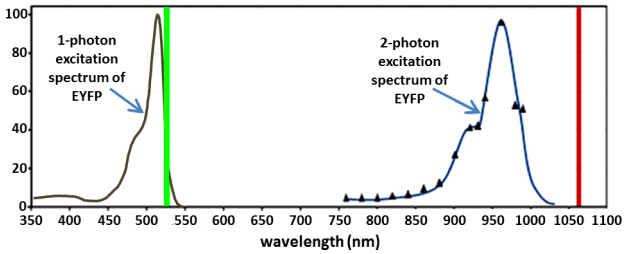

Figure 2. (color online) The normalized 1- and 2-photon excitation spectra of EYFP. The excitation wavelength of 1064 nm and its second harmonic (532 nm) are marked by vertical red and green lines, respectively. (adapted from [28])

overnight at room temperature (RT). After addition of 2 mL TETBS300 (20 mM Tris, 300 mM NaCl, 5 mM EDTA, 0.05% Tween-20, pH 7.5) the solution was kept overnight at RT. To remove unbound oligonucleotides AuNP were centrifuged 30 min at 13200 rpm, the supernatant was removed, the residue dissolved in TETBS 300 and the step repeated twice.

EYFP was modified with DNA as described in an earlier publication [26]. Briefly, 200 μL EYFP (200 μM, 40 nmol, 1 eq.) were reduced with 60 μL DTT (1 M, 60 μmol, 1500 eq.) for 2 h at 23^{o}C. Simultaneously 100 μL amino-cDNA (100 μM, 10 nmol, 1 eq.) was modified with 100 μL sSMCC (46 mM, 4.60 μmol, 460 eq.) for 2 h at 23^{o}C to yield maleimide-cDNA. After purification with NAP5 and NAP10 columns, both solutions were combined and incubated overnight at 4^{o}C. The reaction mixture was concentrated and the buffer changed to 20 mM Tris, pH 8.3 before purification with anion exchange chromatography using a MonoQ 5/50 (GE Healthcare). Signals containing desired product were identified using UV-Vis spectroscopy and native TBE-polyacrylamid gel electrophoresis. To form EYFP-modified AuNP 38.5 μL AuNP-DNA (5.20 nM, 0.20 pmol, 1 eq.) were incubated with 2.67 μL EYFP-cDNA (1.87 μM, 5 pmol, 25 eq.) at room temperature overnight [27]. The resulting conjugate was analyzed with agarose gel electrophoresis.

In our experiment we first constructed a gold cluster complex using EYFP decorated AuNPs together with larger diameter bare AuNPs (Fig. 1). The cluster structure was formed by mixing two droplets of solution containing the two different types of nanoparticles (12 nm and 70 nm) on the atomically flat (100) surface of a silicon wafer. Figures 1 (a)-(d) show a sketch of a single EYFP decorated AuNP, a SEM image of a cluster of such nanoparticles, a sketch of an asymmetric AuNP dimer with EYFPs in the vicinity of the gap, and an SEM image of such clusters, respectively. Au is chosen due to its matching plasmon resonance of 515-560 nm with the SH wavelength of 532 nm, belonging to the irradiation laser of 1064 nm.

Our experiment is based on the idea that EYFP is sensitive to 1064 nm radiation neither linearly nor nonlinearly as can be seen from Fig. 2, since the linear and two-photon absorption bands lie between 430-550 nm and 850-1030 nm, respectively [28]. It is of essential importance to our experiment that there exists a significant shift between twice the one-photon and the two-photon excitation band maxima of EYFP, so that direct two-photon excitation of EYFP by irradiation at 1064 nm is avoided. We experimentally confirmed that; and the details are provided in the next section. So that when irradiated with 1064 nm of light the EYFP molecule can generate a fluorescence signal only if 1064 nm light were up-converted to 532 nm by the asymmetric AuNP cluster. The linear emission band maximum of EYFP is located at 529 nm which is very close to SH signal from the laser.

As we can see from Fig. 1(b), there are areas where smaller nanoparticles decorated by EYFP. We used an inverted microscope's (Zeiss model Axiovert 200) 63X (1.4 NA) objective to identify these areas. Areas with the highest concentration of EYFP were identified by scanning a 532 nm DPSS laser (Cobolt model Samba), and detecting the maxima of the fluorescence signal.

In Fig. 3, a scheme of experimental setup is displayed. We used a cw Nd:YAG laser (Cobolt model Rumba) with wavelength of $\lambda = 1064$ nm and 500 mW output power as excitation source. The NIR signal was delivered from the back port of microscope, resulting in an intensity of 40 MW/cm^2 on the sample. Resulting fluorescence from the clusters was registered by a spectrometer (Andor models Shamrock 750 spectrograph + Newton 971 EMCCD) in corporation with a long-pass dichroic mirror cutting off the backscattered 1064 nm signal and reflecting a band of 532-750 nm.

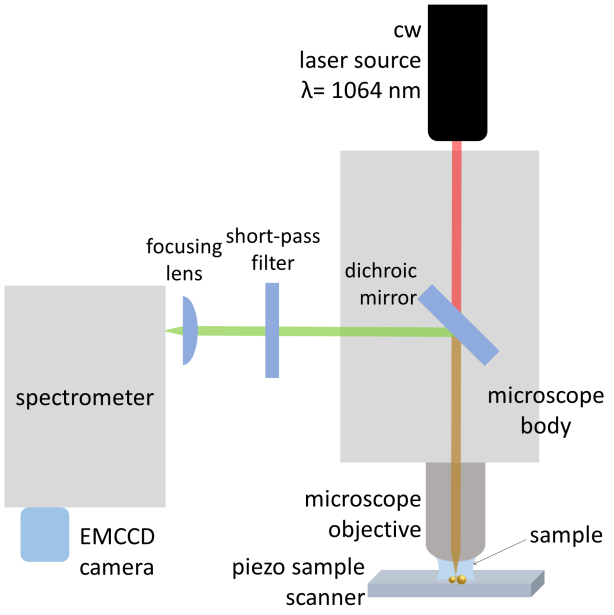

Figure 3. (color online) The experimental setup consists of a cw Nd:YAG laser with $\lambda = 1064$ nm, a long-pass dichroic mirror, a microscope objective, sample, a focusing lens, a short-pass filter (cut-off at 800 nm), a spectrometer with an EMCCD camera.

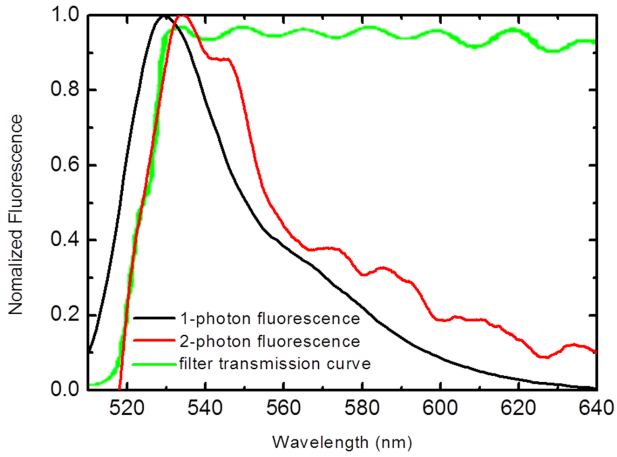

Figure 4. (color online) The fluorescence spectra of EYFP excited both by one-photon (black) and plasmon induced two-photon processes (red) obtained from the asymmetric clusters.

B. Experimental Results

First step in our experiments involved the certification that the direct two-photon excitation of EYFP is avoided by 1064 nm laser irradiation. We have performed control measurements on the clusters of EYFP decorated 12 nm AuNPs in the absence of 70 nm AuNP cluster using the same excitation power as the experiments involving both clusters. The measurements yielded no two-photon fluorescence signal from 12 nm AuNP clusters hosting EYFP molecules. As a second control experiment, we tested SHG activity of the 70 nm AuNP clusters in the absence of 12 nm EYFP AuNP clusters, and similarly observed no SHG converted signal.

Fig. 4 presents the EYFP fluorescence data obtained from EYFP molecules that are sandwiched in-between plasmonic asymmetric structures. The red curve corresponds to fluorescence from such aggregates under 1064 nm illumination. The black curve is the fluorescence obtained by a combination of halogen lamp and a FITC filter set (Zeiss) for a comparison. The green curve is the transmission curve belonging to the dichroic mirror used in this experiment. As expected, the plasmon induced two-photon fluorescence was much weaker compared to the linear fluorescence, by an order of 10^{-12}. This is quite comprehensive since in two-photon excitation, the fluorescence signal originates from only a single or a few molecules sandwiched right in the gap of a AuNP cluster, whereas the linear fluorescence signal originates from all the EYFP molecules besides those whose fluorescence may be quenched by the AuNPs, yet quenching effects both the sandwiched and non-sandwiched molecules equally. A slight shift of fluorescence maximum from the linear emission band maximum of EYFP at 529 nm to ∼535 nm, and a low level modulation of the fluorescence band towards longer wavelengths can be observed. This is a consequence of the transmission properties of the dichroic mirror as the green curve in Fig. 4 suggests. The importance of asymmetry was tested by control experiments in which same size (∼12 nm) nanoparticles were let to form symmetric AuNP clusters, from which a fluorescence signal upon NIR illumination was absent. This confirms that asymmetry of the plasmonic structure plays a crucial role for achieving second harmonic response from plasmonic structures.

Next, we demonstrate that the EYFP molecules are responsible for the enhancement of the SH production due to presence of Fano resonances, as well as reporting the generated 2ω plasmon-polariton (PP) oscillations. We also discuss the assisting role of the hybridization in SH conversion process. Here ω represents the drive frequency corresponding to $\lambda = 1064$ nm excitation wavelength.

The extinction peak of a single 70 nm AuNP is at about $\lambda_1 \cong 510$ nm which is quite far away from $\lambda = 1064$ nm, the wavelength of the excitation laser we use. This mode is scarcely affected by the diameter of the AuNP. When AuNPs are brought together, they hybridize to yield plasmon resonances at longer wavelengths [29]. As an example, in Fig. 5, we present the hybridized spectrum of three 70 nm AuNPs at different sizes, 110 nm, 60 nm and 12 nm. This is one of the possible scenarios taking place at the interface, where a 12 nm AuNP (decorated with molecules) goes in between two larger AuNPs. The low-lying resonance shifts to 580 nm and its tail reaches longer wavelengths. The scattering cross-section grows from 0.44 nm^2 to 726 nm^2. This effect is proposed to be used for wide spectrum conversion in solar cells [30],

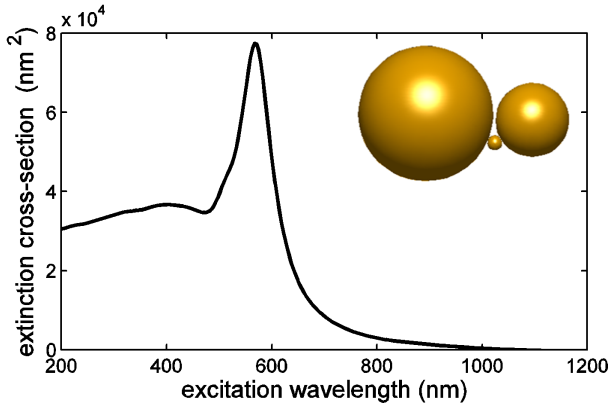

Figure 5. (color online) The extinction cross-section of three hybridized 70 nm AuNPs. The first PP mode, mode 1 with resonance peak at $\lambda_1 = 580$ nm, has an extended tail at the drive wavelength of $\lambda = 1064$ nm. The second PP mode, mode 2, has resonance peak at $\lambda_2 = 400$ nm. Due to the strong localization of the plasmon polarization field, two PP excitations in mode 1 oscillating at $\lambda = 1064$ nm combine to generate a $\lambda/2 = 532$ nm oscillation in the mode 2. Even though, SHG at $\lambda/2 = 532$ nm is off-resonant with λ_2, insertion of a molecule with an absorption peak at $\lambda_{abs} = 514$ nm enhances the SHG (see Fig. 6) substantially.

and gives rise to increased absorption of the incident radiation. Hybridization also assists SHG by shifting the second plasmon excitation peak from 270 nm, for single AuNP, to 400 nm in hybrid (aggregate) AuNPs.

In our experiment, in contrast to larger AuNPs, 12 nm AuNPs require smaller separations (e.g. $\sim$0.3 nm) to express a similar hybridization. This is due to the relatively small spatial extension of the plasmonic excitations. Moreover, the presence of molecules surrounding the 12 nm AuNPs inhibits the hybridization. Hence, one does not observe SHG from 12 nm AuNPs aggregates alone due to the weakness of the hybridization, in addition to the centrosymmetric nature of such particles.

III. THEORY

In two recent theoretical works [12, 13] 3D boundary element method (MNPBEM) simulations demonstrate that second harmonic generation in plasmonic resonators can be enhanced by using the Fano resonances. In these simulations, the retardation effects are taken into account, where it is confirmed that the retardation effects do not play a significant role on the emergence of SHG enhancement.

Nonlinear optical response is strongly modified upon introduction of a coupled quantum emitter which has a small decay rate. When the level spacing of the quantum emitter is resonant with the exact frequency of 2ω, SHG can be suppressed several orders of magnitude. Transparency induced by the Fano resonance, similar to linear case, does not allow the excitation of the second harmonic mode. In contrast, when quantum level spacing is chosen to be in the close proximity of 2ω (e.g. $\omega_{eg} = 2.04\omega$), SHG can be enhanced 2 orders of magnitude. Such an enhancement occurs since the path interference effects cancel nonresonant terms (See Eq. (8) below) and bring the nonlinear conversion to resonance [12]. In the following part, we discuss the enhancement mechanism within the framework of Fano resonance. From our simulations we argue that such an enhancement scheme is in charge of the observed highly enhanced SHG in our experiment.

A previously published k-space spectroscopy experiment [31] revealed that the mechanism of the SHG process in plasmonic resonators is as follows. The field is strongly localized in terms of PP oscillations (ω). Two of such PP oscillations combine to produce a single high frequency (2ω) PP. SH photons (at 2ω) originate from the radiative-decay of this PP excitation [32, 33]. Therefore, the Hamiltonian for the process can be written as

$$H_{sh} = \hbar\chi^{(2)}\left(\hat{a}_2^\dagger \hat{a}_1 \hat{a}_1 + \hat{a}_1^\dagger \hat{a}_1^\dagger \hat{a}_2\right). \tag{1}$$

Here, $\hat{a}_1$ is the driven PP mode, and $\hat{a}_2$ is the PP mode in which SH plasmon excites, and $\chi^{(2)}$ is proportional to the SH dielectric susceptibility. In hybridized AuNPs system, as in Fig. 5, $\lambda_1 = 580$ nm and $\lambda_2 = 400$ nm correspond to resonances a_1 and a_2, ($\omega_1 < \omega_2$), respectively. 1064 nm (ω) radiation excites $\lambda_1 = 580$ nm PP mode and SH plasmon is created in $\lambda_2 = 400$ nm PP mode. We note that, SH plasmon cannot be created in the driven $\hat{a}_1$ PP mode since the excitations are to be presented with the same operator $\hat{a}_1$ and energy conservation inhibits such a term.

Normally, SHG process would be in resonance if the second PP mode ($\hat{a}_2$) would be resonant to $\lambda_2 = 1064/2 = 532$ nm. However we show that due to existence of path interference effects, $\lambda_2 = 400$ nm mode can behave as if it is resonant to 532 nm wavelength. Including the diagonal ($\hat{a}_i^\dagger \hat{a}_i$) and AuNP-molecule interaction ($\hat{\rho_{eg}} \hat{a}_i$) terms to the Hamiltonian in Eq. (1), one obtains the equations of motion [6]

$$\dot{\alpha}_1 = (-i\omega_1 - \gamma_1)\,\alpha_1 - i2\chi^{(2)}\alpha_1^*\alpha_2 - if_1\rho_{ge} + \epsilon_p e^{-i\omega t} \tag{2}$$

$$\dot{\alpha}_2 = (-i\omega_2 - \gamma_2)\,\alpha_2 - i\chi^{(2)}\alpha_1^2 - if_2\rho_{ge} \tag{3}$$

$$\dot{\rho}_{ge} = (-i\omega_{eg} - \gamma_{eg})\,\rho_{ge} + i\,(f_1\alpha_1 + f_2\alpha_2) \times (\rho_{ee} - \rho_{gg}) \tag{4}$$

$$\dot{\rho}_{ee} = -\gamma_{ee}\rho_{ee} + i\left[(f_1\alpha_1^* + f_2\alpha_2^*)\rho_{ge} - c.c.\right] \tag{5}$$

where $\alpha_{1,2} = \langle \hat{a}_{1,2} \rangle$ describe the PP field, $\rho_{ee}(\rho_{ge})$ are diagonal (off-diagonal)matrix elements of (EYFP) molecule with e, g referring to the excited ground states. The 1064 nm laser field drives the first plasmon mode with frequency ω e.g. $\epsilon_p e^{-i\omega t}$. Damping rates of the PP models are about $\gamma_1, \gamma_2 \sim 0.1$ PHz, decay rate of

molecule is about $\gamma_{ee} = 3\gamma_{eg} \sim 0.1$ THz and f_c represents the AuNP-EYFP molecule coupling.

As verified in an earlier work [12] with time evolution simulations of Eqs. 2-5, the steady state solutions of variables has long time behavior

$$\alpha_1 = \tilde{\alpha}_1 e^{-i\omega t}, \alpha_2 = \tilde{\alpha}_2 e^{-i2\omega t} \quad (6)$$

$$\rho_{eg} = \tilde{\rho}_{eg} e^{-i2\omega t}, \rho_{ee} = \tilde{\rho}_{ee} \quad (7)$$

where the variables with tilde are constants. In order to demonstrate the physics (path interference) underlying in the enhancement/suppression scheme using analytical expressions; we neglect the coupling of $\hat{a}_1$ mode to the quantum emitter. Using Solutions (6)-(7), one obtains the simple equation

$$\tilde{\alpha}_2 = \frac{i\chi^{(2)}}{\frac{|f_c|^2 y}{i(\omega_{eg}-2\omega)+\gamma_{eg}} - [i(\omega_2 - 2\omega) + \gamma_2]} \tilde{\alpha}_1^2 \quad (8)$$

for the steady state. Both path interference effects can be simply read from Eq. 8. When ω_{eg} is chosen to satisfy

$$|f_c|^2 y(\omega_{eg}-2\omega)+(\omega_2-2\omega)\left[(\omega_{eg}-2\omega)^2+\gamma_{eg}^2\right] = 0, \quad (9)$$

the $\tilde{\alpha_2}$ generation can be brought to resonance

$$\tilde{\alpha}_2 = -i\chi^{(2)}\tilde{\alpha}_1^2/\gamma_2 \quad (10)$$

even λ_2 =400 nm is off-resonant with SH frequency $\lambda/2$=532 nm.

In Fig. 6, we show that presence of a molecule of level spacing ω_{eg} ≅514 nm (for EYFP), SHG is enhanced about 10^3 times with respect to the no-molecule case. Simulations, depicted in Fig. 6, are obtained by time evolving Eqs. (2)-(5) without neglecting the coupling of $\hat{a}_1$ mode to the quantum emitter. In deriving Eq. (8), we make such negligence merely since we are able to demonstrate the act of path interferences. For the case presented in Fig. 6, $\hat{a}_1$ mode interacts even stronger with the quantum emitter.

The SH conversion takes place at the hot-spots of two (or more) MNPs, due to $\sim 10^5$ factor of field enhancement, wherein dipole-like charge distribution occurs. Regarding the SH process, charge distributions (or electromagnetic field they generate) exhibit symmetry restrictions [34]. The factor $\chi^{(2)}$ in Eq. (1) is an overlap integral $\chi^{(2)} = \int d^3r E_2(r) E_1^2(r)$, where $E_1(r)$ and $E_2(r)$ are the spatial extents of polarization fields that belong to a_1 and a_2 plasmon-polariton modes, respectively. Such a standard overlap integral can be obtained after elimination of the operators responsible for other participated processes, e.g. inter-band transitions [34–39]. The driven mode $E_1(r)$ has a dipole-like behavior, thus $E_1^2(r)$ has an even parity at the hot-spot. For the integral $\chi^{(2)}$ not to vanish: either (i) SH mode $E_2(r)$ must have an even character (e.g. quadruple) or (ii) the two AuNPs surrounding the hot-spot must have non-centrosymmetric shape with respect to the hot-spot (for incomplete cancelling of the integral). Neither the cluster with 12 nm diameter AuNPs, nor 70-100 nm sized AuNPs cluster do not have quadruple modes at the SH frequency of wavelength 532 nm. Hence, SH conversion does not take place into quadrupole oscillations. There only remains the second case (ii) which is very likely at the interface of the two clusters.

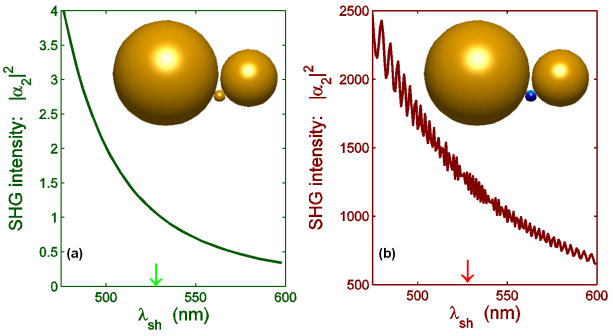

Figure 6. (color online) Enhancement of the SHG in AuNPs by insertion of an EYFP molecule. The path interference effects (See Eq. 8) due to Fano resonances can bring the nonlinear frequency conversion to resonance. For the choice of EYFP, with λ_{eg}=514 nm, SHG is enhanced ∼103 times (b) compared to the no-molecule case (a). (a) Three AuNPs (of sizes 110 nm, 70 nm and 12 nm) interact. (b) The small AuNP (blue) is decorated with EYFP molecule and interacts with larger AuNPs. Arrows indicate the position of the frequency (532 nm) where SH conversion takes place in our experiment.

The combined effects, i) improved cross-section due to hybridization, ii) conversion enhancement due to Fano resonance, and iii) use of non-centrosymmetric clusters, makes SHG observable in our experiment even when using a cw laser. Plasmonic nonlinear conversion of light can be a feasible route for achieving single/few molecule activation due to its strong localization and extremely high efficiency depending on the careful choice of plasmonic-molecular system construction. Simple building blocks for such systems can be localized surface plasmon polariton supporting metal nanoparticles and their hybrids with fluorescent molecules.

SHG takes the form of emerging oscillations of higher order (quadrupole and higher) plasmon modes due to coupling while the primary (dipole-like) mode, as the primary mode is being driven by an external field. The multipolar nature of the generated SH polarization results in strong confinement of this field to the near-field and poor coupling to the far-field. When a fluorescent molecule that has absorption band in the SH frequency of the drive field is placed in the vicinity of the plasmonic system, it can efficiently absorb SH field and reradiate due to its finite electronic lifetime in the form of a dipole radiation, and hence couple effectively to the far-field. So such a fluorescent molecule can be used as a reporter of SHG.

IV. CONCLUSIONS

In summary, we experimentally show that it is possible to excite few EYFP molecules located at the gaps of asymmetric AuNP aggregates by plasmonically converted excitation of NIR photons to their SH visible counterparts by using a cw laser excitation source. We observe the fluorescence of EYFP centered at 529 nm as an asymmetrically constructed (different sized) AuNP aggregate, accommodating the EYFP molecule in the interparticle gaps, is radiated with 1064 nm photons from a cw laser source. Within the light of our numerical simulations, we show that the EYFP molecules are responsible for enhancing the SHG process (due to Fano resonances) [12] 3 orders of magnitude as well as reporting the converted frequency to the far-field. The calculated enhancement factor (of about 1250 at 532 nm in Fig. 6) successfully accounts for the observed SHG under cw excitation in our experiment when compared to a typical SHG experiment performed by using ultra-fast lasers [38] regarding the values of the peak illumination intensities (40 MW/cm^2 in our case and 60 GW/cm^2 in an earlier work[40] yielding a ratio of 1250, i.e. same as the calculated enhancement factor) on the sample. Besides the substantial enhancement due to Fano resonances, hybridization of larger sized AuNPs also works for the account of SH conversion. Shift in the extinction spectrum due to dimerization provides stronger absorption at longer wavelengths (e.g. at 1064 nm). Additionally, the second resonance of AuNPs (at a shorter wavelength of 270 nm) shifts to around 400 nm that is closer to the SH frequency which is at 532 nm. This provides a two sided enhancement by hybridization. When the asymmetry is also accounted, these three effects cooperate to enable the observation of SH signal using a cw laser.

We also present here a theoretical framework based on coupling of classical (plasmons) and quantum oscillators (fluorescing molecules) that explains how such strong nonlinear cross-sections can be possible. The summary of our finding is presented in Eq. (8). We show that coupling of EYFP is not only useful as a reporter molecule but does also have a dramatic effect on the enhanced second harmonic cross-section. In a detailed study [12] of our theoretical model (Eq. (8)), we further demonstrate using 3D boundary element simulations that the pronounced enhancement phenomenon is almost unaffected from retardation effects.

We would like to point that we do not observe the SHG signal directly, but the fluorescence of the EYFP molecule due to strong absorption of the SHG signal by the EYFP. In our interpretation this is due to the fact that the EYFP molecules are well within the Frster radius of the plasmonic AuNPs resulting in a highly effective Frster resonant energy transfer (FRET) of the SHG polarization to the molecule. As a final note, we would like to mention that research on nonlinear behavior of plasmon excitations is finding its niche in diverse applications ranging quantum optical applications such as single-photon switches and single-photon transistors owing to the fact that coupling of plasmon excitation to low dimensional materials with quantum mechanical properties, such as graphene, yields pronounced nonlinear behavior [41] with strong plasmon field enhancement [42], as well as molecular spectroscopy such as Coherent anti-Stokes Raman scattering using Fano resonances to yield single-molecule sensitivity [43]. In a recent work, we show that the pronounced plasmonic activity can further be boosted by coupling of two or more quantum oscillators to plasmonic resonators, interestingly in an unlimited fashion (in principle to the point of divergence), when the strengths of inter-particle interactions and the energy level spacing for quantum oscillators are chosen carefully [13].

ACKNOWLEDGMENTS

The research leading to these results has received funding from: the European Union's Seventh Framework Programme FP7/2007-2013 under grant agreement nr. 270483; Middle East Technical University BAP-08-11-2011-129 grant; Bilim Akademisi - The Science Academy, Turkey BAGEP 2013 award (A.B.). A.B. acknowledges support from TÜBİTAK grants nr. 113F239 and nr. 113F375. M.E.T. and D.T. acknowledge support from TÜBİTAK grants nr. 112T927 and nr. 114F170. This work was undertaken while one of the authors (M.E.T.) was in residence at Bilkent University with the support provided by Oğuz Gülseren.

[1] W. R. Browne and B. L. Feringa, Annu. Rev. Phys. Chem. **60**, 407 (2009).
[2] D. Xiang, Fabrication and utilization of mechanically controllable break junction for bioelectronics. PhD dissertation, Aachen University (2012).
[3] B. Xu and N. J. Tao, Science **301**, 1221 (2003).
[4] A. Gourdon, Eur. J. Org. Chem. **1998**, 2797 (1998).
[5] M. Kauranen, and A. V. Zayats, Nature Photonics **6**, 737 (2012).
[6] S. Palomba, M. Danckwerts and L. Novotny, J. Opt. A: Pure Appl. Opt. **11**, 114030 (2009).
[7] A. Manjavacas, F. J. Garca de Abajo and P. Nordlander, Nano Lett. **11**, 2318 (2011).
[8] R. D. Artuso and G. W. Bryant, Nano Lett. **8**, 2106 (2008).
[9] E. Waks and D. Sridharan, Phys. Rev. A **82**, 043845 (2010).
[10] P. Weis, J. L. Garcia-Pomar, R. Beigang and M. Rahm, Opt. Express **19**, 23573 (2011).
[11] M. E. Taşgın, Nanoscale **5**, 8616 (2010).

[12] D. Türkpençe, G. B. Akgüç, A. Bek, and M. E. Taşgın, J. Opt. **16**, 105009 (2014).

[13] M. E. Taşgın, Divergent nonlinear optical response of three resonator system via Fano resonances. Preprint at http://arxiv.org/abs/1404.3901 (2014).

[14] J. Butet et al., Phys. Rev. B **86**, 075430 (2012).

[15] K. Thyagarajan, J. Butet and O. J. F. Martin, Nano Lett. **13**, 1847 (2013).

[16] J. Berthelot et al., Opt. Express **20**, 10498 (2012).

[17] G. F. Walsh, and L. D. Negro, Nano Lett. **13**, 3111 (2013).

[18] U. Hohenester and A. Trugler, Comput. Phys. Commun. **183**, 370 (2012).

[19] J. J. Storhoff, R. Elghanian, R. C Mucic, C. A. Mirkin and R. L. Letsinger, J. Am. Chem. Soc. **120**, 1959 (1998).

[20] W. Haiss, N. K. Thanh, J. Aveyard and D. Fernig, Anal. Chem. **79**, 4215 (2007).

[21] J. Turkevich, P. C. Stevenson and J. A. Hillier, Faraday Soc. **11**, 55 (1951).

[22] B. V. Enüstün and J. Turkevich, J. Am. Chem. Soc. **85**, 3317 (1963).

[23] I. Ojea-Jimenez, F. M Romero, N. G. Bastus and V. Puntes, The J. of Phys. Chem. C **114**, 1800 (2010).

[24] J. Kimling, M. Maier, B. Okenve, V. Kotaidis, H. Ballot and A. Plech, The J. of Phys. Chem. B **110**, 15700 (2006).

[25] P. Hazarika, F. Kukolka and C. M. Niemeyer, Angew. Chem. **110**, 6827 (2006).

[26] F. Kukolka and C. M. Niemeyer, Org. Biomol. Chem. **2**, 2203 (2004).

[27] C. M. Niemeyer, B. Ceyhan and P. Hazarika, Angew. Chem. **42**, 5766 (2003).

[28] G. A. Blab, P. H. M. Lommerse, L. Cognet, G. S. Harms, and T. Schmidt, Chem. Phys. Lett. **350**, 71 (2001).

[29] P. Nordlander, C. Oubre, E. Prodan, K. Li and M. I. Stockman, Nano Lett. **4**, 899 (2004).

[30] M. C. Günendi, İ. Tanyeli, G. B. Akgüç, A. Bek, R. Turan and O. Gülseren Opt. Express **21**, 18344 (2013).

[31] N. B. Grosse, J. Heckmann and U. Woggon, Phys. Rev. Lett. **108**, 136802 (2012).

[32] A. Bouhelier, R. Bachelot, G. Lerondel, S. Kostcheev, P. Royer and G. P. Wiederrecht, Phys. Rev. Lett. **95**, 267405 (2005).

[33] In our experiment, SHG is reported to far-field by fluorescent molecules.

[34] C. C. Neacsu, G. A. Reider and M. B. Raschke, Phys. Rev. B **71**, 201402(R) (2005).

[35] P. Senet, J. Chem. Phys. **105**, 6471 (1996).

[36] F.P Lohner and A. A. Villaeys, Surf. Sci. **422**, 17 (1999).

[37] W. L. Schaich, Phys. Rev. B **61**, 10478 (2000).

[38] G. Bachelier, J. Butet, I. Russier-Antoine, C. Jonin, E. Benichou and P. F. Brevet, Phys. Rev. B **82**, 235403 (2010).

[39] A. Liebsch, Phys. Rev. Lett. **61**, 1233 (1988).

[40] G. Bautista, M. J. Huttunen, J. Makitalo, J. M. Kontio, J. Simonen and M. Kauranen, Nano Lett. **12**, 3207 (2012).

[41] M. Gullans, D. E. Chang, F. H. L Koppens, F. J. García de Abajo and M. D. Lukin, Phys. Rev. Lett. **111**, 247401 (2013).

[42] S. Thongrattanasiri and F. J. García de Abajo, Phys. Rev. Lett. **110**, 187401 (2013).

[43] Y. Zhang, Y. R. Zhen, O. Neumann, J. K. Day, P. Nordlander and N. J. Halas, Nat. Commun. **5**, 4424 (2014).